Demonstration of laser action in a pseudorandom medium

Jin-Kyu Yang,[1] Svetlana V. Boriskina,[2] Heeso Noh,[1] Michael J. Rooks,[1] Glenn S. Solomon,[3] Luca Dal Negro,[2,a)] and Hui Cao[1,a)]
[1]*Department of Applied Physics, Yale University, New Haven, Connecticut 06520-8482, USA*
[2]*Department of Electrical and Computer Engineering and Photonics Center, Boston University, Boston, Massachusetts 02215-2421, USA*
[3]*Joint Quantum Institute, NIST and University of Maryland, Gaithersburg, Maryland 20899, USA*

(Received 7 August 2010; accepted 20 September 2010; published online 29 November 2010)

We demonstrated lasing in localized optical resonances of deterministic aperiodic structures with pseudorandom morphologies. The localized lasing modes in two-dimensional arrays of air nanoholes in GaAs membranes occur at reproducible spatial locations, and their frequencies are only slightly affected by the structural fluctuations in different samples. A numerical study on the resonances of the passive systems and optical imaging of lasing modes enabled us to interpret the observed lasing behavior in terms of distinctive localized resonances in the two-dimensional pseudorandom structures. © *2010 American Institute of Physics*. [doi:10.1063/1.3519844]

Unlike conventional lasers that utilize mirrors or periodic structures to trap light, random lasers rely on the multiple scattering of light in disordered media for optical feedback and light confinement.[1–3] A major limitation to device applications of random lasers is the lack of control and reproducibility of the lasing modes, namely, the frequencies and spatial locations of lasing modes are unpredictable, varying randomly from sample to sample. Here, we propose to solve this problem by engineering lasing modes in deterministic structures with pseudorandom aperiodic order. The deterministic aperiodic structures, which can be made by the standard nanofabrication techniques, provide the design and fabrication reproducibility required by many practical applications.

Different from random structures, deterministic aperiodic structures (DASs) are defined by the iteration of simple mathematical rules, rooted in symbolic dynamics and prime number theory, which possess very rich spectral features.[4] DAS can be implemented in physical systems as diverse as dielectric multilayers,[5–8] nanopillars,[9,10] and nanoparticle arrays.[11–13] The structural complexity of DASs is measured by their spatial Fourier spectra, which are discrete (singular) for quasiperiodic systems, singular-continuous, or absolutely continuous for pseudorandom structures of increasing complexity. In the recent years, there have been detailed studies on lasing in one-dimensional (1D) and two-dimensional (2D) quasiperiodic photonic media.[14–19] However, structures with absolutely continuous Fourier spectra or pseudorandom DAS have not been investigated so far. In this paper, we demonstrate laser action in 2D pseudorandom media with robust localized lasing modes occurring at reproducible spatial locations and frequencies. We anticipate that the study of lasing in pseudorandom DAS can result in the engineering of multifrequency coherent light sources suitable for planar integration with photonic chips.

The primary example of the pseudorandom DAS is the Rudin–Shapiro (RS) sequence.[4] In a two-letter alphabet, the RS sequence can be obtained by the iteration of the inflation: $AA \rightarrow AAAB$, $AB \rightarrow AABA$, $BA \rightarrow BBAB$, and $BB \rightarrow BBBA$. This inflation method has recently been generalized from 1D sequence to 2D by alternating the 1D inflation map along the orthogonal directions.[20] According to this rule, we can deterministically assign the positions of scattering objects (spheres, cylinders, etc.) across a 2D array once their minimum separation has been chosen. Following this approach, we have fabricated in a free-standing GaAs membrane 2D arrays of air holes arranged in a RS sequence. A 190-nm-thick GaAs layer and a 1000-nm-thick $Al_{0.75}Ga_{0.25}As$ layer are grown on a GaAs substrate by molecular beam epitaxy. Three InAs quantum wells are embedded in the GaAs layer. The RS pattern was written on a 300-nm-thick electron-beam resist ZEP layer with the electron-beam lithography. Then, the pattern was transferred into the $Al_{0.75}Ga_{0.25}As$ layer by chlorine-based inductive coupled plasma reactive ion etching with the ZEP layer as the mask. The ZEP layer is subsequently removed in an oxygen plasma cleaning process. Finally, the $Al_{0.75}Ga_{0.25}As$ layer is selectively etched in a dilute HF solution. Figure 1(a) shows the scanning electron microscope (SEM) image of a 2D array of air holes arranged in the RS sequence in the free-standing GaAs membrane. The air holes have the square shape with the side length $d = 330$ nm. The edge to edge separation of adjacent air holes is 50 nm. The total size of the pattern is about 25×25 μm^2, containing 2048 air holes. 2D Fourier transform

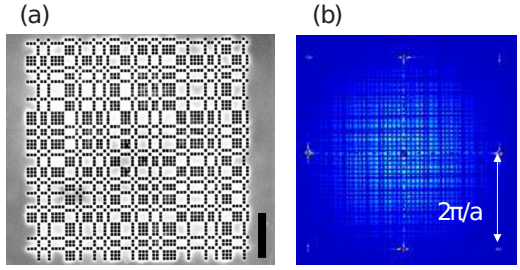

FIG. 1. (Color online) (a) SEM image of a 2D array of air holes arranged in the Rudin–Shapiro sequence in a free-standing GaAs membrane. The black vertical bar is 5 μm. (b) Reciprocal space representation of the structure obtained by Fourier transform of the SEM image. The nine spots around the boundary correspond to the reciprocal vector of square lattice with the lattice constant $a = 380$ nm.

a)Authors to whom correspondence should be addressed. Electronic addresses: dalnegro@bu.edu and hui.cao@yale.edu.

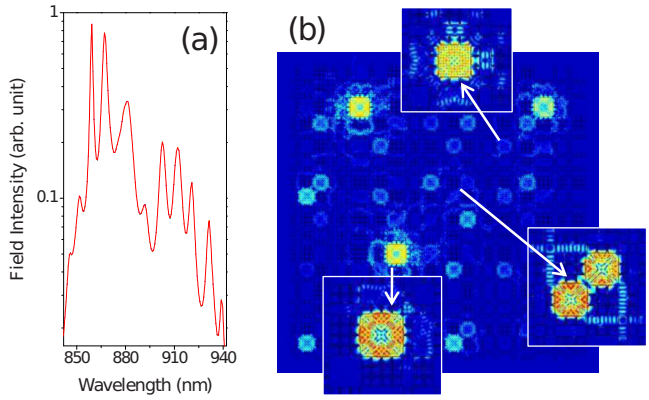

FIG. 2. (Color online) (a) Calculated field intensity inside the structure vs wavelength after short excitation pulses are launched at random locations across the structure. (b) Calculated spatial distribution of electric field intensity (in logarithmic scale) across the RS slab. The insets are the magnified view of resonant modes. The top and left insets are two localized modes at $\lambda=859.2$ and 867.1 nm, respectively. The right inset shows a coupled resonance at $\lambda=867.2$ nm.

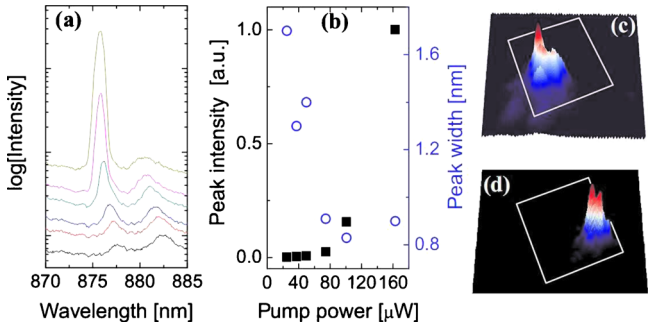

FIG. 3. (Color online) (a) Measured emission spectra at different pumping levels for the RS pattern shown in Fig. 1. (b) Intensity and width $\Delta\lambda$ of the lasing peak vs the incident pump power. (c) Image of the lasing mode. (d) Image of another lasing mode at a different position of the structure.

of the structure produces the spectrum shown in Fig. 1(b), which corresponds to the far-field diffraction pattern. Unlike a quasiperiodic structure with discrete Bragg peaks,[14] the RS structure features a large density of spatial frequency components that form nearly continuous bands. As the system size increases, the spectrum approaches the continuous Fourier spectrum of a white-noise random process.

To investigate the resonant modes of the 2D RS structure in a slab geometry, we performed numerical calculation using the three-dimensional (3D) finite-difference time-domain (FDTD) method. The structural parameters used in the simulations were identical to those of the fabricated sample in Fig. 1(a). We considered the transverse electric (TE) field, namely, the electric field parallel to the slab, because experimentally the laser emission is TE polarized. Optical pulses, with a center wavelength of 880 nm and a spectral width of 30 nm, were launched at randomly selected locations across the pattern. Figure 2(a) is the calculated spectrum of electromagnetic field inside the structure after the excitation pulse left. It contains many resonant modes of distinct frequencies. The spatial distribution of electric field intensity, shown in Fig. 2(b), illustrates that the resonant modes are localized at different positions of the structure. The top and bottom insets in Fig. 2(b) show two strongly localized modes at wavelengths $\lambda=859.2$ and 867.1 nm. Their quality (Q) factors are 570 and 200, respectively. The right inset shows a coupled resonance with $\lambda=867.2$ nm and $Q=300$. Because of its flat Fourier spectrum, the RS structure can support many localized modes, each having a well-defined frequency and position. The Q values of these localized modes are limited by the vertical leakage of light out of the slab.

In the lasing experiments, the samples were cooled to 10 K in a continuous-flow liquid helium cryostat and optically pumped by a mode-locked Ti:sapphire laser (pulse width of ~200 fs, center wavelength of ~790 nm, and pulse repetition rate of ~76 MHz). A long working distance objective lens with a numerical aperture of 0.4 was used to focus the pump light to the structure at normal incidence. The diameter of pump spot on the sample was about 2 μm. The pump spot was moved across the sample to excite localized modes at different positions. The emission from the sample was collected by the same objective lens. The emission spectrum was measured by a 0.5 m spectrometer with a liquid nitrogen cooled coupled charged device (CCD) array detector. Simultaneously, the spatial distribution of the emission intensity across the sample surface was imaged by a TE-cooled CCD camera.

Figure 3(a) shows the evolution of emission spectrum with increasing pump power. Two spectral peaks were observed at low pump. One of them grew rapidly with increasing pump power above a characteristic threshold. Figure 3(b) shows the threshold behavior of the peak intensity versus the incident pump power P. We observed that the spectral width $\Delta\lambda$ of the peak also decreased dramatically with increasing P. Above threshold, the hot carrier effect, produced by the short pump pulse, prevented a further reduction of $\Delta\lambda$, and at higher P, it caused a slight increase of $\Delta\lambda$. This is because the carrier distribution kept changing in time during the short lasing period following the pump pulse. Consequently, the refractive index changes in time, causing a continuous redshift of lasing frequency.[21,22] In our time-integrated measurement of lasing spectrum, the transient frequency shift results in a broadening of the lasing line. Such broadening increases with the hot carrier density and becomes dominant at the highest pump power.

To map the spatial profile of the intensity of this lasing mode, we have used a bandpass filter to block the pump light and imaged the spatial distribution of the emission intensity on the sample surface. The image in Fig. 3(c) reveals a hot spot of laser emission on top of a broad background of (amplified) spontaneous emission within the pumping area. It is evident that the lasing mode is localized inside the RS pattern whose boundary is marked by the square in Fig. 3(c). The lateral dimension of the lasing mode is approximately 2 μm, which agrees well with the size of localized modes in our numerical simulation. When we shifted the pump spot across the sample, the lasing modes changed in terms of locations, frequencies, and spatial profiles. Figure 3(d) shows the intensity distribution of a lasing mode excited at a different position in the structure. This mode exhibits two regions of intense laser emission, suggesting that it originates from a coupled resonance, in agreement with the numerical calculation shown in the right inset in Fig. 2.

To prove the reproducibility of lasing modes in the pseudorandom DAS, we fabricated three identical RS patterns on the same wafer. Figure 4(a) shows the lasing spectra of three patterns when the same area was optically pumped. We observed the same lasing peaks with a slight shift in wavelength. More quantitatively, the wavelength shift is within

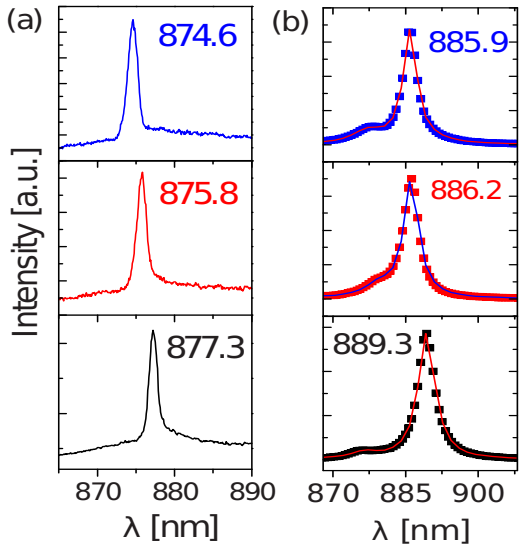

FIG. 4. (Color online) (a) Measured lasing spectra of three RS patterns fabricated on the same wafer. The incident pump power is (from bottom to top) 149, 435, and 522 μW. The wavelengths λ of lasing modes are written next to the peaks in units of nm. (b) Calculated excitation spectra of those structures that were directly extracted from the SEM images. The mode wavelengths are written in units of nm.

0.3% of the lasing wavelength. Although the lasing peak blueshifted with increasing pump power below and near the lasing threshold [Fig. 3(a)], it remained at almost the same spectral position once the pump power exceeded the lasing threshold. The wavelength shift was caused by a change in the carrier density, which was clamped above the lasing threshold (a result of gain saturation). The three spectra in Fig. 4(a) were taken at the pump powers well above the lasing thresholds; thus, the shift of lasing wavelengths was caused by a slight structural variation due to limited fabrication accuracy. To simulate the wavelength shift, we extracted the structures from the top-view SEM images and input them to the 3D FDTD calculation.[23] We launched short excitation pulses within the pump area and found the resonant modes of similar wavelength. As shown in Fig. 4(b), the mode wavelength indeed shifts slightly from pattern to pattern. The resonant wavelengths are not exactly equal to the measured ones; they differ by approximately 1%. This difference is attributed to the limited accuracy in determining the value of refractive index due to low temperature and hot carrier effect. Nevertheless, both the overall trend of wavelength shift and the intensity distribution of the modes well match our experimental data.

In summary, we found that pseudorandom arrays of air holes in GaAs membranes can support spatially localized optical resonances that exhibit clear lasing behavior in the presence of gain. Moreover, we proved that the spectral positions of these lasing modes are reproducible and robust against the structural fluctuations in different samples due to fabrication imperfections. The deterministic aperiodic systems provide an alternative approach from random media and photonic crystals for the engineering of multifrequency coherent light sources and complex cavities amenable to predictive theories and technology integration.

We acknowledge inspiring discussions with Professor Douglas Stone and Professor Eric Akkermans. This work was partially supported by the NSF (Grant No. DMR-0808937), the U.S. Air Force (Award No. FA9550-10-1-0019), and the NSF Career (Award No. ECCS-0846651). A part of sample fabrication was carried out at the Center for Functional Nanomaterials, Brookhaven National Laboratory, which is supported by the U.S. Department of Energy, Office of Basic Energy Sciences, under Contract No. DE-AC02-98CH10886.

[1] H. Cao, in *Progress in Optics*, edited by E. Wolf (Elsevier, Amsterdam, 2003), Vol. 45, p. 317.
[2] M. A. Noginov, *Solid-State Random Lasers*, Springer Series in Optical Sciences Vol. 105 (Springer, New York, 2005).
[3] D. Wiersma, Nat. Phys. **4**, 359 (2008).
[4] E. Maciá, Rep. Prog. Phys. **69**, 397 (2006).
[5] M. Kohmoto, B. Sutherland, and K. Iguchi, Phys. Rev. Lett. **58**, 2436 (1987).
[6] W. Gellermann, M. Kohmoto, B. Sutherland, and P. C. Taylor, Phys. Rev. Lett. **72**, 633 (1994).
[7] L. Dal Negro, C. J. Oton, Z. Gaburro, L. Pavesi, P. Johnson, A. Lagendijk, R. Righini, L. Colocci, and D. S. Wiersma, Phys. Rev. Lett. **90**, 055501 (2003).
[8] L. Moretti, I. Rea, L. Rotiroti, I. Rendina, G. Abbate, A. Marino, and L. De Stefano, Opt. Express **14**, 6264 (2006).
[9] S. V. Zhukovsky, D. N. Chigrin, and J. Kroha, J. Opt. Soc. Am. B **23**, 2265 (2006).
[10] S. Boriskina, A. Gopinath, and L. Dal Negro, Opt. Express **16**, 18813 (2008).
[11] L. Dal Negro and N. Feng, Opt. Express **15**, 14396 (2007).
[12] A. Gopinath, S. Boriskina, N. N. Feng, B. M. Reinhard, and L. Dal Negro, Nano Lett. **8**, 2423 (2008).
[13] A. Gopinath, S. Boriskina, B. Reinhard, and L. Dal Negro, Opt. Express **17**, 3741 (2009).
[14] M. Notomi, H. Suzuki, T. Tamamura, and K. Edagawa, Phys. Rev. Lett. **92**, 123906 (2004).
[15] K. Nozaki and T. Baba, Appl. Phys. Lett. **84**, 4875 (2004).
[16] S.-K. Kim, J.-H. Lee, S.-H. Kim, I.-K. Hwang, Y.-H. Lee, and S.-B. Kim, Appl. Phys. Lett. **86**, 031101 (2005).
[17] K. Nozaki and T. Baba, Jpn. J. Appl. Phys., Part 1 **45**, 6087 (2006).
[18] X. Xu, H. Chen, and D. Zhang, Appl. Phys. B: Lasers Opt. **89**, 29 (2007).
[19] L. Mahler, A. Tredicucci, F. Beltram, C. Walther, J. Faist, H. E. Beere, D. A. Ritchie, and D. S. Wiersma, Nat. Photonics **4**, 165 (2010).
[20] L. Dal Negro, N. N. Feng, and A. Gopinath, J. Opt. A, Pure Appl. Opt. **10**, 064013 (2008).
[21] G. Pompe, T. Rappen, M. Wehner, F. Knop, and M. Wegerner, Phys. Status Solidi B **188**, 175 (1995).
[22] F. Jahnke and S. W. Koch, Phys. Rev. A **52**, 1712 (1995).
[23] H.-G. Park, S.-H. Kim, S.-H. Kwon, Y.-G. Ju, J.-K. Yang, J.-H. Baek, S.-B. Kim, and Y.-H. Lee, Science **305**, 1444 (2004).